GRAPHENE-COATED PYROLYTIC CARBON

FOR LITHIUM BATTERIES AND OTHER APPLICATIONS

by

MING ZHANG

(Under the Direction of Ian R. Hardin)

ABSTRACT

In this work, we utilized cotton fabric as a template to create macro sheets of graphene. The cotton fabric was dipped into a graphene/pyrene- derivative suspension. The graphene-coated cotton textile was then annealed at a high temperature in a quartz tube furnace under argon flow. During the annealing process, the gaps between separated graphene sheets were "soldered" by the "glue" molecules (aromatic molecular surfactants) to form graphene-coated pyrolytic carbon. The result was a graphene "skin" created on the pyrolytic carbon scaffold that is flexible graphene coat and can contribute relatively high capacity to a lithium battery sandwich. This occurs because of porous structure of graphene sheets and the high surface area of the pyrolyzed carbon with a shell-core structure. This novel, facile, and low-cost method can be expanded to applications on other carbon-rich materials such as peanut shells, wood waste and other cellulosic waste materials.

INDEX WORDS: Graphene, Pyrolytic carbon, Lithium ion batteries, Storage capacity

GRAPHENE-COATED PYROLYTIC CARBON FOR LITHIUM BATTERIES AND OTHER APPLICATIONS

by

MING ZHANG

B.S., East China University of Science and Technology, China, 2004

M.S., University of Science and Technology of China, China 2008

A Thesis Submitted to the Graduate Faculty of The University of Georgia in Partial Fulfillment of the Requirements for the Degree

MASTER OF SCIENCE

ATHENS, GEORGIA

2011

GRAPHENE-COATED PYROLYTIC CARBON

FOR LITHIUM BATTERIES AND OTHER APPLICATIONS

by

MING ZHANG

Major Professor: Ian R. Hardin

Committee: Suraj Sharma
Jason Locklin

Electronic Version Approved:

Maureen Grasso
Dean of the Graduate School
The University of Georgia
August 2011

DEDICATION

This thesis is dedicated to my wife (Qin Sun), dear grandparents (Guanglan Shan and Haitian Li), my dear parents (Meiling Li and Rongsheng Zhang), my friends and Jesus for their forever love and support.

ACKNOWLEDGEMENTS

This thesis would never have been completed without help and support of people who are gratefully acknowledged here.

Foremost, sincere thanks to my major advisor, Dr. Ian R. Hardin, for his great insight in the proposal of the research and his substantial assistance and guidance throughout my entire course of study and research at the University of Georgia.

Special thanks to my committee members, Dr. Suraj Sharma and Dr. Jason Locklin, for their valuable suggestions, ideas and comments in the research.

I am very grateful to the faculty, staff, and graduate students, especially Susan Wilson from the Department of Textiles, Merchandising and Interiors for their cooperation and help.

I would like to extend my thanks to Dr. Xiangwu Zhang from NC State University for instrumentation support.

My deep appreciation goes to my lovely families for their endless love, support and confidence on me.

I give thanks to my God upon my every remembrance of you

Table of Contents

Page

Acknowledgements v

List of Tables viii

List of Figures ix

Chapter

1 Introduction 1

1.1 Statement of Problem.....4

1.2 Objective of Study 5

2 Literature Review.....6

2.1 Introduction of Lithium-ion Batteries.....6

2.2 Mechanism of Lithium-ion Batteries.....7

2.3 Carbon-based Anode Materials.....9

2.4 One-dimensional Carbon Anode Materials 9

2.5 Two-dimensional Carbon Anode Materials 12

2.6 Three-dimensional Carbon Anode Materials.....13

2.7 Properties of Graphene and Its Applications 15

3 Materials and Methods.....20

3.1 Materials 20

3.2 Preparation of Graphene Suspension.....20

3.3 Preparation of Graphene-coated Pyrolytic Carbon 21

3.4 Characterization 21

4 Results and Discussions 23

4.1 Fluorescence Spectrum of Graphene/ Py-SO_3 Suspension 23

4.2 Morphological Structure of Graphene 24

4.3 Conductance Measurement of Graphene-coated Pyrolytic Carbon 26

4.4 SEM and EDX Analysis of Graphene-coated Pyrolytic Carbon Fibers 29

4.5 Capacitance Measurements of Graphene-coated Pyrolytic Carbon 30

5 Conclusions and Future Work 32

5.1 Conclusions 32

5.2 Future Work 33

References 34

List of Tables

Pages

Table 4.1: The changes of resistance of the graphene-coated pyrolytic carbon samples with the graphene loadings..... .27

Table 4.2: The weight add-on from the graphene/pyrene suspension after drying.....28

Table 4.3: The total percent weight loss after annealing…….....28

List of Figures

Pages

Figure 1.1: Illustration of the approach to the intermolecular condensation of graphene and pyrene into graphene networks on the surface of a fiber..... 3

Figure 2.1: Nokia Li-ion Battery 6

Figure 2.2: Schematic operating principle of a typical rechargeable LIB 8

Figure 2.3: Carbon nanotube structure.....10

Figure 2.4: Graphene structure 12

Figure 2.5: Three-dimensional carbon material.....13

Figure 3.1: Illustration of the position of points used for resistance measurement on the sample.... ……..22

Figure 3.2: Diagram of the light-emitting diode circuit.....22

Figure 4.1: Molecular structure of 1,3,6,8- pyrenetetrasulfonic acid tetrasodium salt hydrate.....23

Figure 4.2: Fluorescence spectroscopy used to monitor the direct exfoliation process in the presence of pyrene molecules….....24

Figure 4.3: (A) Atomic force microscopy (AFM) images of the graphene sheets on a mica substrate.....25

(B) is the section analysis of the AFM image in (A) along the black line.....25

Figure 4.4: (A) an incomplete light-emitting diode.....26

(B) and (C) a light-emitting diode circuit closed by cotton/graphene hybrids or graphene-coated pyrolytic carbon…….....27

(D) photograph of graphene-coated pyrolytic carbon.....27

(E) graphene-coated pyrolytic carbon stretched by tweezers 27

Figure 4.5: SEM images (A) and (B) of graphene-coated pyrolytic carbon fibers.....29

(C) and (D) cross section of a broken graphene-coated pyrolytic carbon fiber.....30

Figure 4.6: EDX analysis of the surface of a graphene-coated pyrolytic carbon fiber.....30

Figure 4.7 Cyclibility of graphene-coated textile at 50 mA/g current density 31

Chapter 1

Introduction

Graphene is a one atom-thick material made up of sp^2-bonded carbon atoms. Its unique properties include high electrical and thermal conductivity, the quantum Hall effect, massless transportation properties, and strong mechanical properties [1-11]. Among several possible applications, the use of graphene as an electrode in lithium batteries is very promising because of graphene's relatively low-cost and accessibility. However, a graphene anode alone provides relatively low lithium storage capacity and has an unstable charge and discharge cycle performance. This is a problem to overcome before the commercialization of graphene based electrodes is feasible. Recently, several different nanomaterials, including various carbonaceous materials and nanometal/oxides, have been tested as templates to enhance the lithium storage capacity and the cycling performance of the graphene [12-14]. However, because of the high cost, inaccessibility, and the potential nano-toxicity of these template materials, it has been difficult to produce graphene-based electrode materials on a large scale.

Cotton is almost pure cellulose. It is a carbon-rich, cheap, and available on a large scale. The United States is the second largest cotton producer, by far the largest exporter in the world and regularly ships 40 to 60 percent of its yield abroad. US currently accounts for more than 50 percent of the world exported cotton.

The functionalization and modification of traditional textile materials with nanomaterials and nanotechnologies has led to a new revolution. Xin et al reported the functionalization of common cotton fibers with carbon nanotubes (CNTs). Due to the reinforcement and protection

of CNTs, the cotton textiles exhibit enhanced mechanical properties, extraordinary flame retardancy, improved UV-blocking and super water repellent properties [15]. More recently, Cui et al reported that highly electroconductive cotton/carbon nanotube composites can be simply prepared by dipping a cotton fleece (pile) fabric in a carbon nanotube solution. This was successful because of the flexibility of the nanotubes and the strong binding between the carbon nanotubes and the cotton fibers [16]. Graphene also exhibits the good flexibility and electro-conductivity that carbon nanotubes do, but with the added advantage of being potentially much less expensive.

However, little research has been done on the fabrication of graphene-coated textiles, probably due to the difficulty of preparing stable graphene solutions, wrapping the seamless graphene layer on the fibers, and reaggregation of graphene sheets, as well as the complications of pre- and post-treatments. Mullen et al reported that pyrene molecules can not only act as nano-graphene molecules to heal possible defects in the graphene oxides, but can function as electrical ‘‘glue’’, soldering adjacent graphene sheets during the annealing process [17]. In addition, He and colleagues reported a simple and scalable exfoliation approach to produce high-quality graphene suspensions by sonicating graphite in an aqueous solution of hydrophilic pyrene molecules [18]. In the present work (as shown in Figure 1.1), we propose to use cotton fibers as templates where the graphene sheets will be created and wrapped around the fibers. The approach is to immerse cotton fabric in a graphene suspension and “solder” with the nanographene (pyrene derivative) by annealing. The result should be a graphene-coated pyrolytic carbon material. Here, the pyrene derivative plays a double role in the preparation of the material. In the graphene suspension, the pyrene derivative acts as a surfactant to disperse, stabilize and separate the graphite sheets from each other; in the annealing process, it acts as a

"glue" to heal defects and bridge the gap between graphene sheets. Because of the core-shell structure of the graphene-coated pyrolytic carbon, the graphene-coated pyrolytic carbon may exhibit excellent charge/discharge performance, as well as mechanical flexibility.

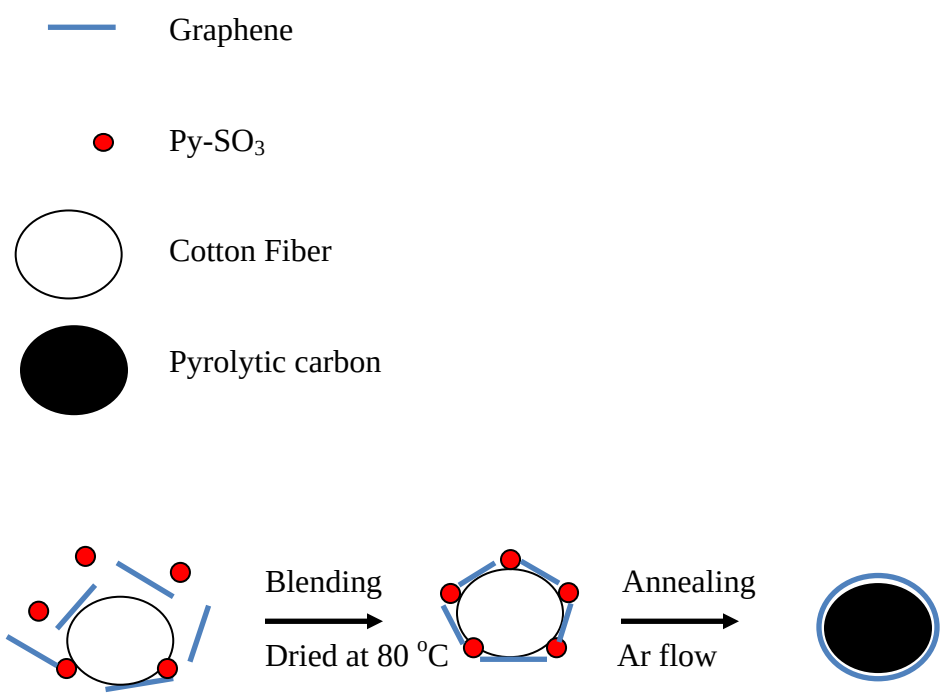

Figure 1.1 Illustration of the approach to the intermolecular condensation of graphene and pyrene into graphene networks on the surface of a fiber.

In the present work, the chemical nature, morphology, and thermal and electrical properties of the graphene-coated pyrolytic carbon were studied by atomic force microscopy (AFM), UV-Vis spectroscopy, scanning electron microscopy (SEM), energy-dispersive X-ray spectroscopy (EDS) and galvanostatic charge-discharge experiments. The primary goal of this work was to produce a facile, low-cost method to prepare graphene-coated pyrolytic carbon

materials for potential applications in energy-storage, electronics, “smart” textiles and perhaps in water treatment.

1.1 Statement of Problem

The performance of rechargeable lithium-ion batteries (LIBs) is totally dependent on the active materials employed for lithium storage in the electrodes. The basic requirements for active materials include high reversible capacity, good structural flexibility and stability, fast Li-ion diffusion, long cycle life, improved safety, low cost, and environmental benignity. In anodes, graphite is the most utilized material for lithium-ion batteries in the industry due to its low and flat working potential (i.e., lower than 0.5 V vs. Li/Li+), long cycle life, and low cost [19-24].

However, most lithium-enriched intercalated compounds of graphite have a ratio of six carbons to one lithium ion, resulting in a less-than-desirable theoretical charge capacity (i.e., 372 $mAh \cdot g^{-1}$) [25-26]. Further advances in current lithium-ion batteries are bottlenecked by limitations associated with electrode materials such as limited capacity, lack of shape flexibility, short cycle life, and poor safety.

Recent progress in electrochemistry, materials science, and solid state chemistry has led to the application of nanomaterials for efficient energy storage in high-performance lithium-ion batteries. To increase energy and power densities as well as the electrochemical performance of lithium-ion batteries, it is necessary to develop novel nanostructured carboneous anode materials.

The purpose of the research was to use cotton, converted to pyrolytic carbon, as the framework for forming a graphene coating, creating a composite material with high conductivity and capacity performance.

1.2 Objective of Study

In this work, we used the cotton fabrics as a template to create a graphene coated pyrolytic carbon nanocomposites which have a shell-core structure. The overall objective of this study was to use graphene sheets to improve the electrochemical performance of pyrolytic carbon materials.

There were several specific objectives of this research, as listed below:

1) Investigate the mechanism of reaction between the pyrene molecules and graphene sheets under the sonication.
2) Investigate the morphological structures of the graphene coated pyrolytic carbon.
3) Investigate the influence of annealing on the electrochemical properties of graphene coated pyrolytic carbon.
4) Investigate the influence of concentration of graphene/pyrene derivative solution on the resistance of graphene coated pyrolytic carbon.

Chapter 2

Literature Review

2.1 Introduction of Lithium-ion Batteries

Rechargeable lithium-ion batteries (LIBs) are very common in portable consumer electronics including cell phones, laptops, and digital cameras, because of their high energy-to-weight ratios, lack of memory effect, and slow self-discharge when not in use [27]. In addition to consumer electronics, lithium-ion batteries are increasingly used in future electric vehicles, hybrid electric vehicles and aerospace applications due to their high energy density [28].

Figure 2.1 Nokia Li-ion Battery

The first person to have come up with the concept of these lithium ion batteries was M.S. Whittingham from the Binghamton University. He used a titanium sulfide and lithium to power a battery he devised in the 1970s [29]. The use of metallic lithium worked fine for the batteries as

far as power was concerned but they posed certain safety issues and concerns and could not be made commercially unless some safer solution was found.

Experimentation was later done on the intercalation technique using and graphite in 1980 by Rachid Yazami at the French National Center for Scientific Research and Grenoble Institute of Technology. This work indicated that lithium intercalation in graphite was indeed a reversible reaction and could be used in the making of rechargeable lithium batteries [30].

In 1991, Sony released the first lithium ion battery on a commercial scale. People took to these batteries instantly and many electronic devices are powered now with the help of these rechargeable batteries. These cells worked on the principle of layered oxide chemistry and used lithium cobalt oxide as a substitute for the previously used lithium metal.

2.2 Mechanism of The Lithium-ion Batteries

The charge/discharge mechanism of LIBs is based on the rocking-chair concept. A typical LIB consists of a cathode (e.g., $LiCoO_2$) and an anode (e.g., graphite), together with an electrolyte-filled separator that allows lithium-ion transfer but prevents electrodes from contacting with each other (Figure 2.2) [31]. When the battery is charging, lithium de-intercalates from the cathode and intercalates into the anode. Conversely, during discharge Li intercalates into the cathode via the electrolyte. During charge/discharge, Li ions flow between the anode and the cathode, enabling the conversion of chemical energy into electrical energy and the storage of electrochemical energy within the battery. The chemical reactions involved in a typical LIB cell are described as follows:

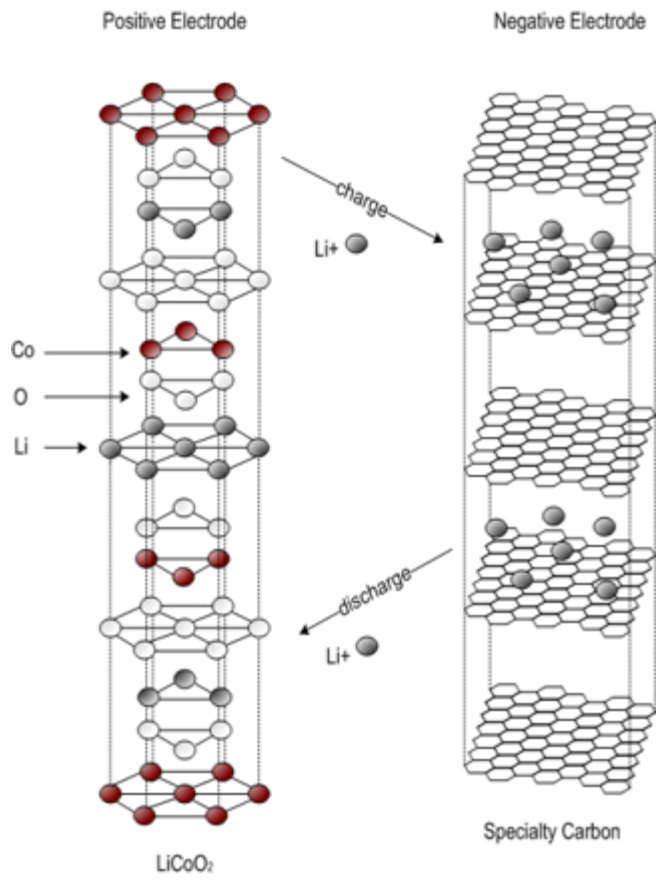

Figure 2.2 Schematic operating principle of a typical rechargeable LIB [32].

The positive electrode half-reaction (with charging being forwards) is:

$LiCoO_2 \quad Li_{1-x}CoO_2 + xLi^+ + xe^-$

The negative electrode half-reaction is:

$xLi^+ + xe^- + 6C \quad Li_xC_6$

The overall reaction has its limits. Over discharge supersaturates the lithium cobalt oxide, leading to the production of lithium oxide, possibly by the following irreversible reaction:

$Li^+ + LiCoO_2 \quad Li_2O + CoO$

Overcharge up to 5.2 Volts leads to the synthesis of cobalt(IV) oxide.

$LiCoO_2 \quad Li^+ + CoO_2$

In a lithium-ion battery the lithium ions are transported to and from the cathode or anode, with the transition metal, cobalt (Co), in Li_xCoO_2 being oxidized from Co^{3+} to Co^{4+} during charging, and reduced from Co^{4+} to Co^{3+} during discharge.

2.3 Carbon-based Anode Materials

Carbon-based anode materials were chosen because of the ability of lithium to intercalate without excess volumetric expansion. High volumetric expansion causes degradation of the battery and a large amount of irreversibility rendering the battery useless for any application with a need for rechargeable energy storage [33].

Carbon-based anode materials are generally categorized into three classes:

(1) one-dimensional carbon;

(2) two-dimensional carbon;

(3) three-dimensional carbon,

2.4 One-dimensional Carbon Anode Materials

The development of one-dimensional nanostructured carbon materials, such as nanotubes, nanowires, and nanofiber, for high-performance LIBs is stimulated by their high surface-to-volume ratio and excellent surface activities. Shortly after the discovery of carbon nanotubes

(CNTs), many researchers studied the interactions of Li vapor with CNTs and measured the corresponding electrochemical properties [34-37].

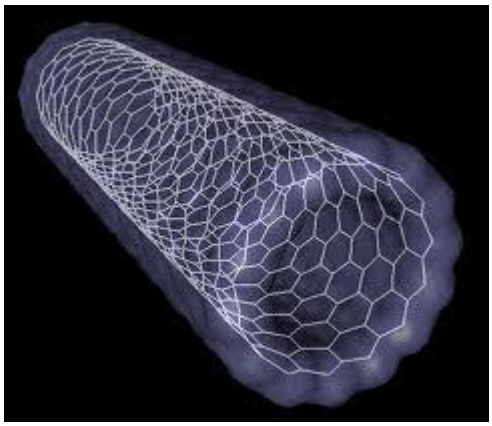

Figure 2.3 Carbon nanotube structure [38].

It was found that CNTs can offer Li intercalation between pseudo-graphitic layers and/or inside central tubes. The small diameters of CNTs can impose strain on the planar bonds of the hexagon. This strain causes de-localization of electrons and makes the structure more electronegative than regular graphitic sheets, which in return increases the degree of Li intercalation. Therefore, the reversible capacities of anodes made from CNTs can exceed 460 $mAh \cdot g^{-1}$and reach up to 1116 $mAh \cdot g^{-1}$ by various post-treatments such as ball milling, acid oxidation, and metal oxide cutting [39-40]. The relatively high capacity of CNTs represents a dramatic improvement over graphite; however, the coulombic efficiency of CNTs was found to be low compared with that of graphite due to the introduction of large structure defects and high voltage hysteresis [41-42]. Numerous research activities on using various CNTs as anodes for rechargeable LIBs have been reported. However, the practical use of CNTs in LIBs is currently limited by their high cost and the relatively long diffusion time for Li insertion/extraction.

Carbon nanofibers (CNFs), synthesized using different methods such as chemical vapor deposition, arc-discharge, template deposition, laser ablation, or electrospinning, can also be used as anodes for rechargeable LIBs. Unlike CNTs, which require a long diffusion time for Li insertion/extraction, the large amount of defects in CNFs, such as lattice and surface defects along the fiber length, are expected to promote fast Li insertion/extraction with theoretical capacities of 400-800 $mAh \cdot g^{-1}$ [43-45]. For example, Wang et al. synthesized porous CNFs with an average diameter of 100 nm and lengths of 2-3 μm by pyrolysis of a conducting polymer in argon, which delivered a reversible capacity of approximately 400 $mAh \cdot g^{-1}$ at 0.5 C and a reversible capacity of 250 $mAh \cdot g^{-1}$ at 10 C with a nearly 100 percent capacity retention after 100 cycles [43]. More recently, CNFs were also prepared using the simple and low cost electrospinning technique and subsequent carbonization processes. These electrospun CNF anode materials can deliver a relatively large reversible capacity of approximately 450 $mAh \cdot g^{-1}$ at 30 $mA \cdot g^{-1}$. Zhang and his coworker improved the electrochemical performance of CNFs by preparing several kinds of porous CNFs via an electrospinning/carbonization process combined with chemical treatments [44]. These porous CNFs have much higher specific surface area and larger pore volume compared with non-porous CNF anodes. The porous structure improved Li-ion diffusion at the electrolyte-electrode interface and added freedom for volume change associated with Li-ion intercalation.

Although one dimensional nanostructured carbons are expected to have higher reversible capacities as well as good cycling stability, they often possess large irreversible capacities, unsatisfactory rate performance, and low volumetric energy density due to the formation of solid electrolyte interface (SEI) and less-compact structure [44].

2.5 Two-dimensional Carbon Anode Materials

Two-dimensional nanomaterials, often referred to as nanosheets or nanofilms, haven't received much attention until the recent reports of applying graphene and its composites.

Graphene is a one atom-thick material made up of sp^2-bonded carbon atoms. It can be produced by either top-down (e.g., the mechanical scotch tape method and chemical exfoliation from graphite) or bottom-up (e.g., chemical vapor deposition) methods. The unique physical and chemical properties of this two dimensional nanomaterial have interested scientists from various fields.

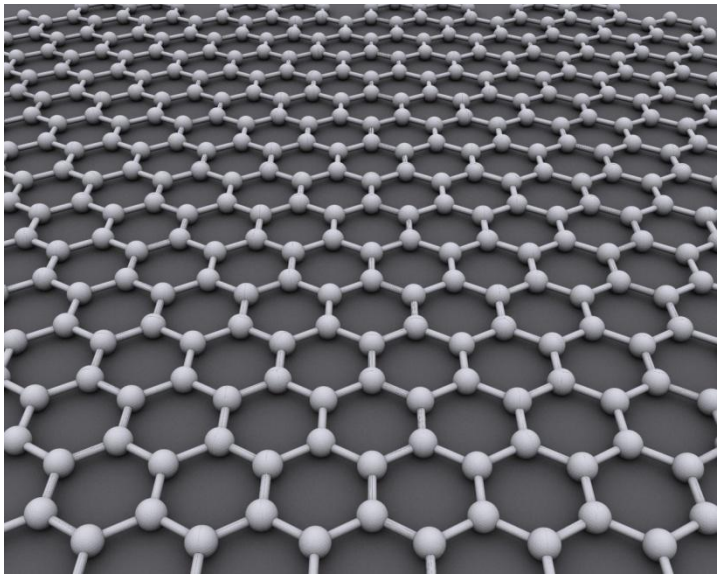

Figure 2.4 Graphene structure [46].

The most intriguing property of graphene is its remarkably high electron mobility and its size-dependent electrical properties, making it a promising material in high-performance electronic devices [47-48]. Optically, graphene shows light absorption from UV to near-infrared

(NIR) regions [49]. It has also been found that graphene oxide (GO) exhibits a size-dependent visible and NIR fluorescence, although the mechanism is not yet fully understood [50]. Graphene contains largely dislocated π-electrons that allow energy transfer from the nearby molecules [51].

Graphene can be used as electrode materials for lithium ion batteries because of its large surface-to-volume ratio, high conductivity, good structural flexibility, and broad electrochemical window [52-57]. In addition, Li can be bound not only on both sides of graphene sheets, but also on the edges and covalent sites of the graphene nanoplatelets. Therefore, it is expected that graphene could overtake its three dimensional counterpart (graphite) for enhanced Li storage in rechargeable LIBs with a capacity of 1000 $mAh \cdot g^{-1}$ or higher.

2.6 Three-dimensional Carbon Anode Materials

Higher rate capability and better cycling performance of LIBs can be achieved by making effective porous carbon electrodes. This is due to the desirable characteristics associated with the high surface area and open structure of porous materials. Porous carboneous materials, with different pore sizes ranging from nanometer to micrometer scale, have attracted much attention as promising anode materials for LIBs [58-59].

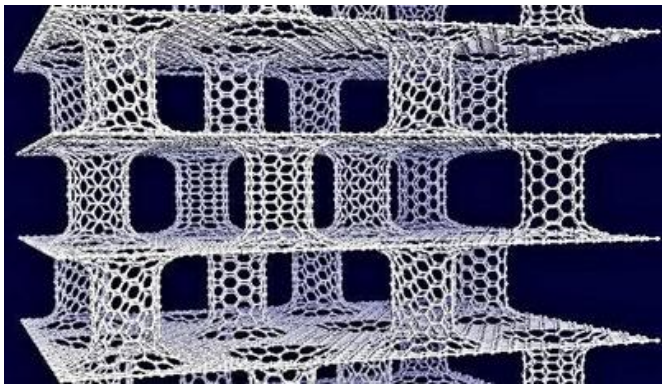

Figure 2.5 Three-dimensional carbon material [60].

Microporous carbons (pore size < 2 nm) have demonstrated larger capacities than traditional graphitic carbons, although in many cases relatively high irreversibilities are also accompanied. For example, Takeuchi et al. used a template method to prepare high-surface area microporous carbons for use as anodes [61]. The prepared microporous carbons displayed a high reversible capacity of 480 $mAh \cdot g^{-1}$, but a large irreversible capacity of 3685 $mAh \cdot g^{-1}$ was observed due to a high hydrogen-to-carbon ratio. In addition, a high capacity fade was also found in the first few cycles, which severely limits the use of these materials as anodes for LIBs. Therefore, further investigations need to be performed to improve the electrochemical performance of these materials by maintaining good capacity retention and reducing irreversible capacity.

In addition to microporous carbons, mesoporous carbons (2 nm < pore size < 50 nm) have been extensively studied as potential anode materials for LIBs. Jiang et al. synthesized 3D ordered mesoporous carbon by using mesoporous silica as a hard template from an impregnation procedure [62]. These anode materials presented a uniform pore size of 7.4 nm and a surface area of 750 m^2/g, and delivered a charge capacity of 616 $mAh \cdot g^{-1}$ with a reversible capacity of 131 $mAh \cdot g^{-1}$ at the first cycle. Zhou et al. improved the capacity of mesoporous carbon materials by using silica SBA-15 as a template [63]. These carbon materials possessed 3D ordered hexagonal structure with uniform pore sizes, high surface areas, and large pore volumes. Anodes made from these carbonaceous materials exhibited a high reversible capacity of 1100 $mAh \cdot g^{-1}$ at the first cycle. However, an irreversible capacity of 2000 $mAh \cdot g^{-1}$ was reported due to the large surface area. After the first cycle, both charge and discharge capacities stayed relatively stable. This should be due to the minimized ion-transport resistance, the localized graphitic structures around the pores and more importantly, the ordered porous structure.

Ordered macroporous carbons (pore size > 50 nm) have also been synthesized using template-based methods to improve the electrochemical performance of anodes in LIBs. For example, colloidal poly(methyl methacrylate) (PMMA) was used as templates by Su et al [64] to prepare ordered macroporous carbons which exhibited a high capacity of 320 $mAh \cdot g^{-1}$ after 60 cycles with a high capacity retention of 98 percent. On the other hand, Stein et al. prepared macroporous CNFs with well-interconnected pore and wall structures using a PMMA colloid-crystal template and obtained a capacity of 260 $mAh \cdot g^{-1}$ at a high current density of 1000 mA/g and a capacity retention of 83 percent after 30 cycles [65]. The relatively good electrochemical performance reveals that 3D macroporous carbons may have the following benefits:

(1) short diffusion pathways for both mobile Li ions and electrons,

(2) large amount of active sites for charge transfer reactions,

(3) reasonable electrical conductivity provided by well-interconnected walls, and

(4) minimized mechanical stress for buffering volume expansion and contraction during lithium insertion/extraction.

However, inherent disadvantages of porous carbon structures are low volumetric energy density and large irreversible capacity. Coating them with other high-capacity components offers a promising strategy for relieving these hurdles.

2.7 Properties of Graphene and Its Applications

Graphene is a promising anode material. Although the capacities of graphene are relatively high, graphene sheets often stack with each other to form multilayers, resulting in losses of high surface area and intrinsic chemical and physical properties. Recently, a strategy of jamming graphene sheets with nanoparticles was used to minimize their aggregation. Both metal

nanoparticles (e.g., Sn and Si) [66-70]and metal oxide nanoparticles (e.g., Co_3O_4, TiO_2, Fe_3O_4, and SnO_2) [71-75] have been used to form graphene composites for this purpose. For example, Yao et al. prepared SnO_2-graphene nanocomposites using the in-situ chemical synthesis method. The prepared nanostructured anodes showed a reversible capacity of 765 $mAh \cdot g^{-1}$ in the first cycle, and the capacity remained at 520 $mAh \cdot g^{-1}$ after 100 cycles [76]. Honma et al. improved the electrochemical performance of SnO_2-graphene nanocomposites by introducing nanopores into reassembled graphene nanosheets in ethylene glycol solution with the presence of SnO_2 nanoparticles [77]. The obtained SnO_2/graphene had layered platelets along with spherical shapes. These SnO_2/graphene electrodes exhibited a high reversible capacity of 810 $mAh \cdot g^{-1}$ at 50 mA/g. After 30 cycles, the capacity was preserved at 570 $mAh \cdot g^{-1}$, indicating 70 percent capacity retention. These values were much larger than those of pure graphene and SnO_2 anodes, and the commercially available graphite. The relatively high capacity retention of the SnO_2/graphene composite is attributed to the dimensional confinement of the graphene component that accommodates the volume expansion upon Li insertion and buffering space formed by pores between SnO_2 and graphene. However, the practical application of this combination is still not feasible because the large-scale production of graphene nanosheets and metal nanomaterials remains a major challenge.

Graphene was initially isolated by mechanical exfoliation, peeling off the top surface of small area of pyrolytic graphite, a method which is not suitable for large-scale application. Another method involves single sheets of graphene oxide which are chemically reduced to graphene after deposition on a silicon substrate, again a method that lends itself to limited applications [78-84].

Recently, a simple and scalable exfoliation approach to produce high-quality single-layer graphene sheets was reported [18]. In a typical experimental procedure, graphite powder was exfoliated by sonicating in an aqueous solution of pyrene molecules that had been functionalized with different water-soluble groups. Highly conductive graphene sheets stabilized in aqueous suspensions were directly produced without requiring toxic reducing agents and expensive solvents. Most importantly, different from other surfactants and polymers that have been used to prevent graphene sheets from aggregation in solution, the pyrene molecules also act as nanographene molecules to heal the possible defects in the graphene sheets during annealing. Remarkably, they also appear to act as electrical ‘‘glue’’ soldering adjacent graphene sheets, such that electric contacts between graphene sheets can be dramatically improved across the film.

Because of quantum size effects and large surface area to volume ratio, nanomaterials have unique properties compared with their larger counterparts [85-89]. However, nanoparticles can be inhaled, swallowed, absorbed through skin and deliberately or accidentally injected during medical procedures. They might be accidentally or inadvertently released from materials implanted into living tissue. Research within the past few years has turned up a range of potential health hazards. For example, the researchers in the University of Texas in the United States found that carbon nanotubes squirted into the trachea of mice caused serious inflammation of the lungs and granulomas (tumour-like nodules of bloated white blood cells in the lining of the lungs), and five of the nine mice treated with the higher dose died [90]. In a similar experiment carried out at the National Institute of Occupational Safety and Health in Morgantown, West Virginia, in the Unites States, researchers not only found granulomas in the lungs, but also damage to mitochondrial DNA in the heart and the aortic artery, and substantial oxidative

damage, both foreshadowing atherosclerosis (hardening of the arteries) [91]. The results, released in 2008, showed that iron oxide nanoparticles caused little DNA damage and were non-toxic. Zinc oxide nanoparticles were slightly worse. Titanium dioxide caused only DNA damage . Carbon nanotubes caused DNA damage at low levels. Copper oxide was found to be the worst offender, and was the only nanomaterial identified by the researchers as a clear health risk.

Pyrolytic carbon is a material similar to graphite, but with some covalent bonding between its graphene sheets as a result of imperfections in its production. Generally it is produced by heating a hydrocarbon nearly to its decomposition temperature, and permitting the graphite to crystallise (pyrolysis) [92-95]. Contrary to the toxicity of some nanomaterials, pyrolytic carbon is in medical use to coat anatomically correct orthopaedic implants as replacement joints. In this application it is currently marketed under the name "pyrocarbon". These implants have been approved by the FDA for use in the hand for metacarpophalangeal (knuckle) replacements [96].

Pyrolytic carbon anode materials for lithium ion batteries have many advantages and disadvantages when compared to graphite. The advantages include higher capacity (per unit mass), good rate capabilities and lower cost of production. The disadvantages that must be resolved before a successful material can be commercialized are the low density, incompatibility with current coating technologies, larger irreversible capacity and hysteresis in the voltage. In addition, a high capacity fade was also found in the first few cycles, which severely limits the use of these materials as anodes for lithium ion batteries.

Some reports have suggested that those problems can be solved by using composite anode materials consisting of a mixture of pyrolytic carbon and graphite [97-101]. These composites have higher rate capabilities and longer cycle lives when compared to pure pyrolytic carbon. As

far as we know, graphene is a kind of monolayer graphite which we believe can take the place of the role that graphite play in the composite anode. In this research, increasing the capabilites and reducing the irreversible capacity of pyrolytic carbons is a primary focus. In order to achieve this goal, a study of the electrochemistry and structure of promising graphene coated pyrolytic carbon materials is presented and correlated to various parameters that can be adjusted during synthesis. We believe that the combination of graphene and pyrolytic carbon can provide lithium ion battery with a high capacity, stable cyclability and low cost.

Chapter 3

Materials and Methods

3.1 Materials

Synthetic graphite powder (<20 mm particle size), and 1,3,6,8-pyrenetetrasulfonic acid (Py-SO_3) tetrasodium salt hydrate from Sigma–Aldrich were purchased and used as received. The cotton fleece fabric (390 g/m^2) was produced in the labs of Cotton Inc. Flame retardant cotton fabrics, including Seminole^{TM} denim twill (442 g/m^2), Cannonball^{TM} canvas (445 g/m^2) and Apache^{TM} khaki twill (252 g/m^2), were donated by Mount Vernon Mills Inc.

3.2 Preparation of The Graphene Suspension

A graphene suspension was synthesized from natural graphite flakes by a method similar to that described by He et al[18]. A typical stock solution of Py-SO_3 with a concentration of 1.0 mg/mL was prepared in deionized water by vigorous stirring for 1 hour. Graphite powder was added to the resultant solutions with a 2:1 weight ratio for the cotton fleece and a 1:1 weight ratio for the other fabrics of the pyrene derivatives to the graphite powder. Direct exfoliation of graphite to graphene sheets was performed by bath sonication of the obtained dispersions for one hour. The exfoliation process was monitored by observing the fluorescence ultraviolet-visible absorption spectrum at the beginning and at the end of the exfoliation period. The resulting gray dispersion was used directly to prepare a graphene-coated textile.

3.3 Preparation of Graphene-coated Pyrolytic Carbon

Graphene sheets were produced on cotton fabric by using a method similar to that described by Cui et al [15] to coat cotton fibers with carbon nanotubes. Fabric specimens were cut 3 cm by 4 cm. The cotton fabric was immersed into the prepared graphene suspension for 15 seconds. The fabric was then dried at 80 ^{o}C for two hours. The annealing process (under inert gas (N_2) flow) was divided into three stages:

1) the temperature was raised from room temperature to 200 ^{o}C and held for 30 minutes;

2) annealing for 20 minutes at 700 ^{o}C ;

3) cooling down to room temperature.

3.4 Characterization:

Graphene sheets: The dispersion of exfoliated graphene sheets was pipetted onto a mica sheet and dried. These sheets were then imaged with a tapping mode Nanoscope IIIa atomic force microscopy (AFM) instrument (Veeco instrument, Santa Barbara, CA, USA). The fluorescence spectrum of the graphite dispersion in Py-SO_3 was monitored using a Cary-Eclipse fluorescence spectrophotometer (Varian, Inc, Palo Alto, CA).

Graphene coated pyrolytic carbon: The morphology, microstructures and energy-dispersive X-ray spectroscopy (EDX) analysis of the graphene-coated pyrolytic carbon were characterized using a field emission gun scanning electron microscope (Philips XL-30).

Capacitance performance: Electrochemical charge/discharge performance of the graphene-coated pyrolytic carbon was evaluated using 2032 button coin cells (Hohsen Corp.)[102] The coin cells were assembled in a high purity argon filled glove box. Charge (lithium insertion) and

discharge (lithium extraction) were conducted using an Arbin automatic battery cycler at a constant current density of 50 mA/g between cut-off potentials of 0.01 and 2.8 V.

Resistance measurements: Figure 3.1 shows the method for resistance measurements. We chose four typical positions on the sample sheet as the measurement points. After annealing, the sample was measured with an ohmmeter. Figure 3.2 shows the light-emitting diode circuit diagram.

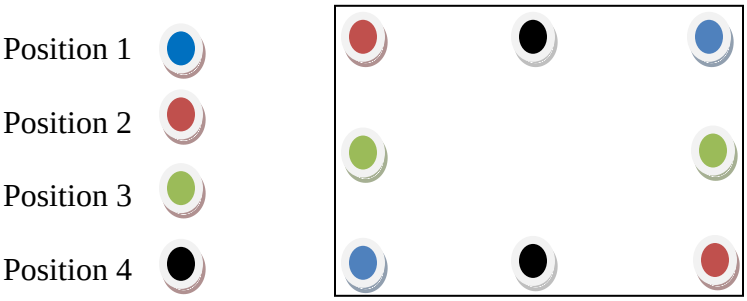

Figure 3.1 Illustration of the positions of the measure points on the sample.

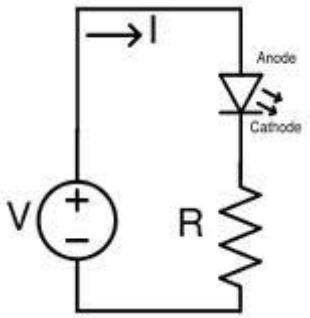

Figure 3.2 The light-emitting diode circuit diagram.

Chapter 4

Results and Discussion

4.1 Fluorescence Spectrum of Graphene/Py-SO_3 Suspension

1,3,6,8-pyrenetetrasulfonic acid tetrasodium salt hydrate is an aromatic molecule that has four benzene rings. It can form an excited dimer, called an excimer, when two monomers are in close proximity (within about 1-2 Å). An excimer is formed if an excited pyrene monomer, during its fluorescence lifetime, interacts in a specific manner with neighboring ground (unexcited) states of pyrene.

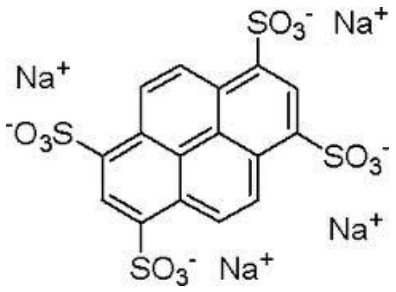

Figure 4.1 Molecular structure of 1,3,6,8- pyrenetetrasulfonic acid tetrasodium salt hydrate

Figure 4.2 shows fluorescence spectra (excited at 340 nm) of a graphene/Py-SO_3 suspension at different sonication periods. Prior to sonication, the spectrum shows a large peak at 500 nm, which was ascribed to the excimer emission of pyrene derivatives [103,104]. We found that the intensity of this peak decreased significantly after one hour of sonication. At the same time, we observed a dramatic increase in the peak at 374nm. This fluorescence behavior is virtually the same as that of the Py-SO_3 aqueous solutions alone when the concentration of Py-

SO_3 is below its critical micelle concentration, suggesting that the fluorescence of the graphene/Py-SO_3 solution is derived by the non-bound (free) Py-SO_3 monomers in the solution.

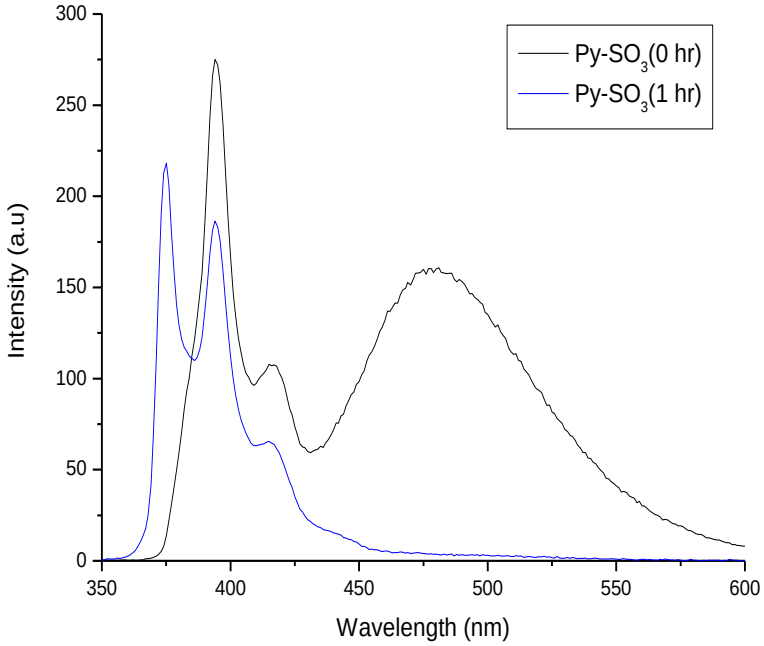

Figure 4.2 Fluorescence spectroscopy used to monitor the direct exfoliation process in the presence of Py-SO_3 molecules.

4.2 Morphological Structure of Graphene

Graphene sheets: Atomic force microscopy (AFM) was used to characterize the graphene sheets obtained by sonication in aqueous solution. AFM is an effective way for the characterization of graphene. Although the graphene is very thin, its morphological features can be determined by AFM and it is possible to estimate the number of graphene layers. Figure 4.3 (A) shows a typical tapping-mode AFM image of graphene/pyrene hybrids deposited on a freshly cleaved mica surface. The width of the graphene patches were in the micrometer range.

The thickness of a single-layer hybrid ranged from 0.5 to 1.3 nm with an average of 0.9±0.4 nm, measured by section analysis, as shown in Figure 4.3 (B). The variation in the thicknesses was attributed to the possible inhomogeneous coverage of Py-SO_3 molecules on the graphene surface, or simply due to the AFM system noise [18]. There were some holes in the surfaces, with diameters ranging from 2 nm to 500 nm randomly arranged on the graphene sheets. It is believed that these holes were caused by sonication and can be partly healed during annealing. The holes, themselves, could actually facilitate capture of lithium ions in battery anodes. Figures 4.2 and 4.3 indicate that the graphene suspension was successfully created by sonication in pyrene aqueous solution.

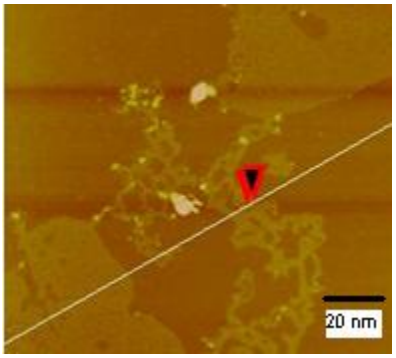

(A)

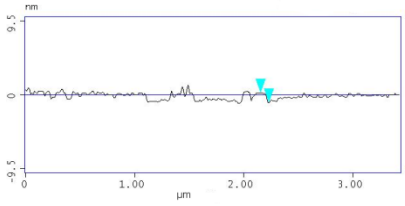

(B)

Figure 4.3 (A) Atomic force microscopy (AFM) images of the graphene sheets on a mica susbtrate. Panel (B) is the section analysis of the AFM image in (A) along the black line. The arrows in the pictures help to indicate the height of the graphene sheet.

4.3 Conductance Measurement of Graphene-Coated Pyrolytic Carbon

Conductance: Figure 4.4 (A) and (B) shows the pictures of the graphene-coated pyrolytic carbon sample, which is flexible and metallic. Figure 4.4 (C)-(E) shows a circuit designed to test the conductivity of graphene-coated pyrolytic carbon samples before and after annealing. The figure shows that annealing improves the conductivity of the sample, which allows the successful operation of the light-emitting diode in the circuit.

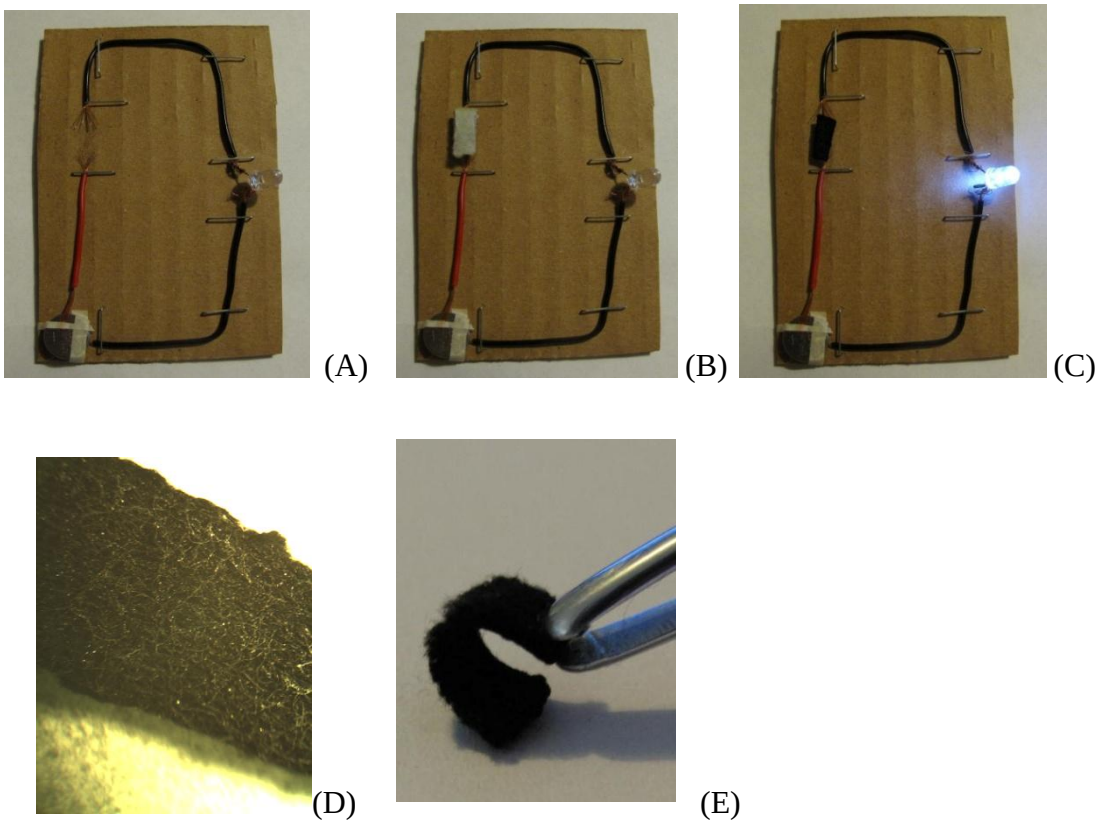

Figure 4.4 (A) an incomplete light-emitting diode; (B) and (C) a light-emitting diode circuit closed by cotton/graphene hybrids or graphene-coated pyrolytic carbon; (D) photograph of graphene-coated pyrolytic carbon; (E) graphene-coated pyrolitic carbon stretched by tweezers.

Table 4.1 presents the changes in electrical resistance with the graphene suspension concentration of various graphene-coated pyrolytic carbon samples prepared by annealing. It demonstrates that the samples show enhanced conductivity with the diluted graphene suspension.

For example, when the concentration of graphene suspension used in sample 4 decreases by half in sample 1, the resistance of sample 4 in position 4 is 27 percent of the conductivity of sample 1 for cotton fleece. The similar trend is observed for other cotton fabrics in Table 4.1. This could be caused by the different ratio between monolayer and multi-layer graphene sheets in the samples. Kim et al found that the mobility of electrons in bilayer graphene is roughly an order of magnitude lower than in a single graphene sheet, which means the monolayer graphene has higher conductivity [105]. This is because graphene's conductivity decreases significantly when more than one layer is present. In sample 1, the amount of the graphene deposit is high and the possibility of forming multi-layer graphene is greater than for sample 4. Table 4.2 shows the weight add-on of the graphene/pyrene suspension after immersion and drying. Table 4.3 gives the total percent weight loss after annealing.

Ohmeter readings of resistance of fabrics					
		Position on fabric			
Fabric	**Treatment**	**1 (Ω)**	**2 (Ω)**	**3 (Ω)**	**4 (Ω)**
Cotton Fleece 1	1.0 mg/ml $PyS0_3$ 0.5 mg/ml graphite	1500	1400	930	1500
2	0.8 mg/ml $PyS0_3$ 0.4 mg/ml graphite	1400	1300	1400	700
3	0.66 mg/ml $PyS0_3$ 0.33 mg/ml graphite	1200	900	930	700
4	0.5 mg/ml $PyS0_3$ 0.25 mg/ml graphite	1000	900	750	400
FR Cotton Khaki	Untreated	2200	2000	1600	1100
	0.5 mg/ml $PyS0_3$ 0.5 mg/ml graphite	1400	900	800	650
	0.4 mg/ml $PyS0_3$ 0.4 mg/ml graphite	1100	800	650	550
	0.3 mg/ml $PyS0_3$ 0.3 mg/ml graphite	550	500	450	350
FR Cotton Denim	Untreated	1100	950	800	650
	0.5 mg/ml $PyS0_3$ 0.5 mg/ml graphite	900	750	650	450
	0.4 mg/ml $PyS0_3$ 0.4 mg/ml graphite	900	750	550	450
	0.3 mg/ml $PyS0_3$ 0.3 mg/ml graphite	450	400	350	250
FR Cotton Canvas	Untreated	900	750	700	600
	0.5 mg/ml $PyS0_3$ 0.5 mg/ml graphite	700	650	550	400
	0.4 mg/ml $PyS0_3$ 0.4 mg/ml graphite	950	650	500	400
	0.3 mg/ml $PyS0_3$ 0.3 mg/ml graphite	600	600	300	250

Table 4.1 The changes of resistance of the graphene-coated pyrolytic carbon samples with the graphene loadings on various cotton fabrics.

Treatment Add-on	Cotton khaki	Cotton denim	Cotton canvas
0.5 mg/ml $PyS0_3$ 0.5 mg/ml graphite	0.003g	0.002g	0.003g
0.4 mg/ml $PyS0_3$ 0.4 mg/ml graphite	0.003g	0.002g	0.002g
0.3 mg/ml $PyS0_3$ 0.3 mg/ml graphite	0.002g	0.002g	0.002g

Table 4.2 The weight add-on from the graphene/pyrene suspension after drying

Percent Weight loss after annealing	Cotton khaki	Cotton denim	Cotton canvas
0.5 mg/ml $PyS0_3$ 0.5 mg/ml graphite	60.5	63	62.5
0.4 mg ml $PyS0_3$ 0.4 mg/ml graphite	41.5	55	56
0.3 mg/ml $PyS0_3$ 0.3 mg/ml graphite	50	60	64

Table 4.3 The total percent weight loss after annealing

4.4 SEM and EDX Analysis of Graphene-Coated Pyrolytic Carbon Fibers

Scanning electron microscopy (SEM) and energy-dispersive x-ray spectroscopy (EDX): Figure 4.5 shows an SEM image of the graphene-coated pyrolytic carbon after annealing. Figures 4.5 A and B show that the graphene sheets formed on the fibers and that the fibers kept the original shape. This indicates that pyrene molecules are successful in "glueing" the graphene sheets to form a seamless membrane on the surface of the fibers during annealing. Figures 4.5 C and D show the cross-section of a broken fiber where the graphene sheets can be seen on the circumference of the cross-section. In Figure 4.6, EDX data indicate that almost 100 percent of the elements are on the surface of the observed fibers are carbon, which means that the oxygen containing groups in the graphene sheet and the Py-SO_3 have almost completely disappeared. This further demonstrates that the graphene sheets are 'soldered' by the fusion of graphene sheets and Py-SO_3 on the fiber surfaces.

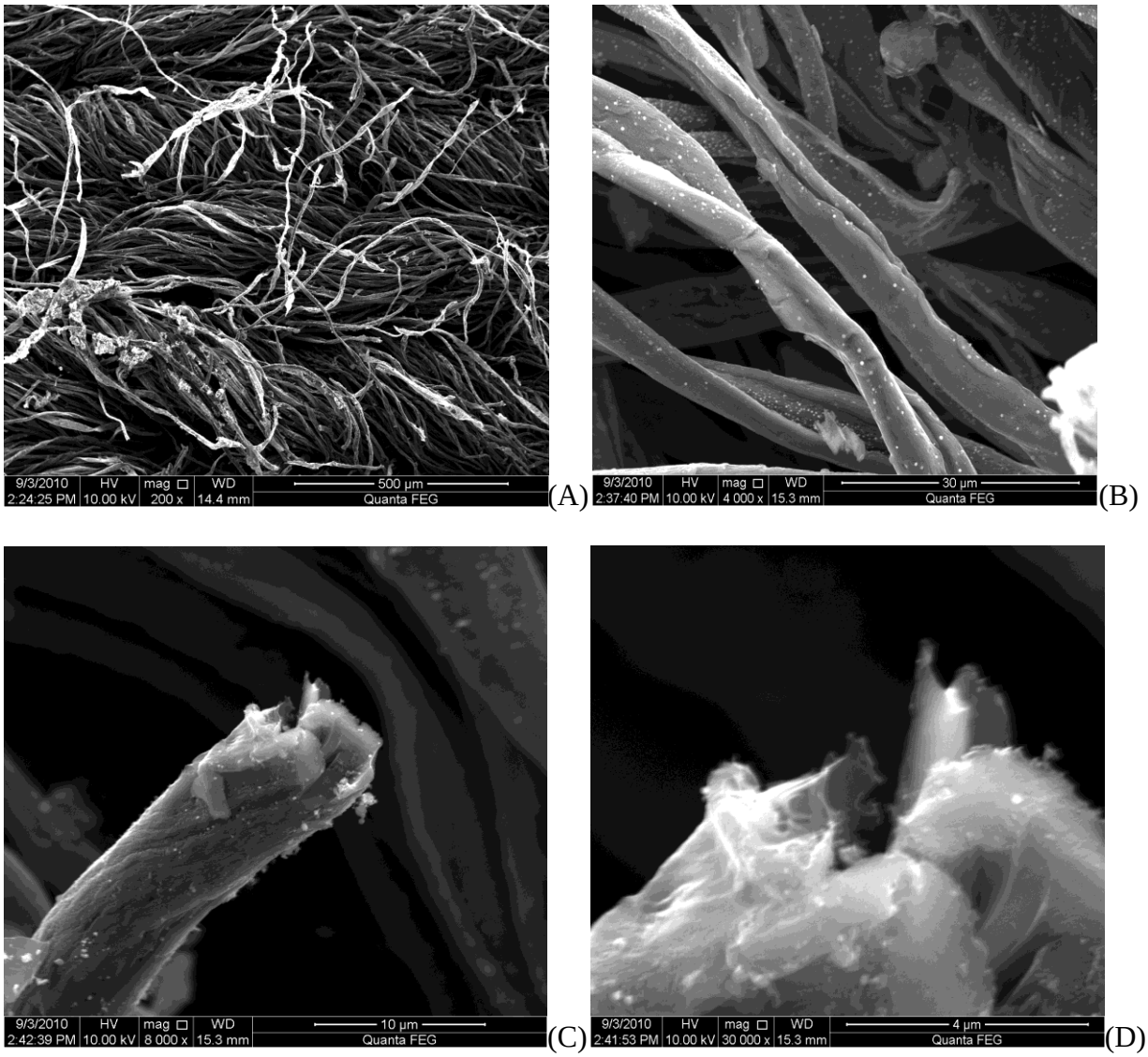

Figure 4.5 SEM images (A) and (B) of graphene-coated pyrolytic carbon fibers; (C) and (D) cross section of a broken graphene-coated pyrolytic carbon fiber.

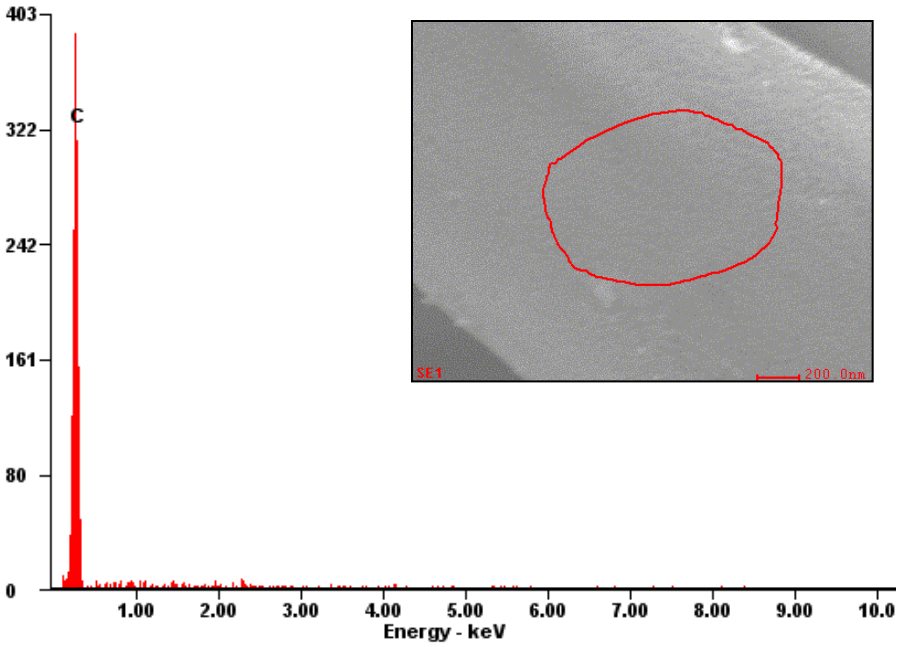

Figure 4.6 EDX analysis of the surface of a graphene-coated pyrolytic carbon fiber; the red circle indicates the area of EDX analysis.

4.5 Capacitance Measurements of Graphene-Coated Pyrolytic Carbon

Capacitance measurements:

Galvanostatic charge-discharge experiments were carried out at a current density of 50 mA g^{-1} within a voltage window of 0.01–2.8 V to evaluate the electrochemical performance of graphene-coated pyrolytic carbon fabric (Figure 4.7). The figure shows that graphene-coated pyrolytic carbon anodes have larger lithium storage capacities than the values reported for graphene paper anodes normally used in lithium batteries. For the latter, the discharge capacity drops sharply from 680 $mAh{\cdot}g^{-1}$ to 84 $mAh{\cdot}g^{-1}$ from the first to the second cycle [106]. For the graphene-coated pyrolytic carbon fabric, about 50 percent of capacity loss was observed in the first cycle, after which the charge-discharge efficiency was above 94 percent from the 2nd cycle to the 50th cycle (Figure 4.7). Notably, the graphene-coated pyrolytic carbon electrode provided a reversible discharge capacity as high as 288 $mAh{\cdot}g^{-1}$ (82.1 % of the capacity on the second

cycle) even after 50 cycles, whereas with the pyrolytic carbon electrode alone rapid degradation of capacitance occurred.

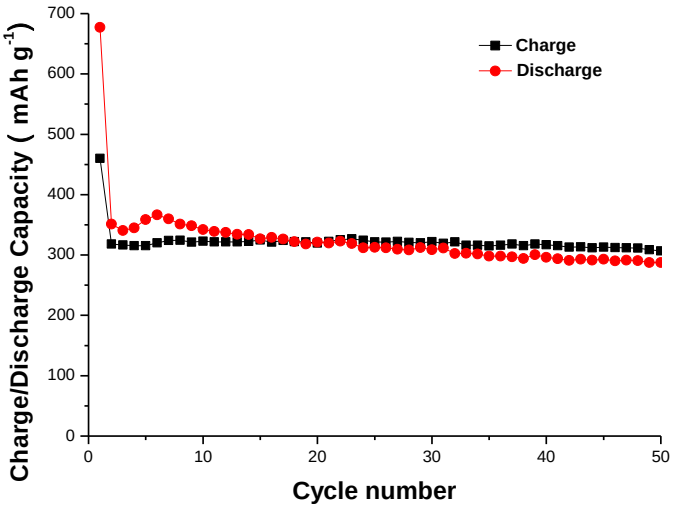

Figure 4.7 Cyclibility of graphene-coated textile at 50 mA/g current density.

It is believed that the remarkable high electrochemical performance of the graphene-coated pyrolytic carbon is due to the porous graphene sheets and the high surface area of pyrolytic carbon fabric. The annealing process dramatically reduced gaps between individual graphene sheets and also improved the electrical contacts between graphene sheets around the fibers. At the same time, the porous structure of graphene allows the lithium ions to penetrate into pyrolytic carbon. Further study is ongoing to determine the exact mechanism for this increased capacity and cycle life, and to improve the formation and performance of the graphene-coated pyrolytic carbon fabric.

Chapter 5

Conclusions and Future Work

5.1 Conclusions

We have successfully created flexible graphene-coated pyrolytic carbon anode materials by fusing graphene sheet by annealing onto cotton fibers, thus creating graphene-coated cotton, or graphene/cotton composites, for the first time.

The novel pyrolytic carbon fabric coated with graphene sheets was characterized by scanning electron microscope (SEM) and energy-dispersive X-ray spectroscopy (EDX).

Due to the extremely high surface area to mass ratio of the electroconductive graphene, it has the excellent cyclability and storage capacity as a anode material to be possible used in the rechargeable lithim-ion batteries.

The novel graphene-coated pyrolytic carbon materials and their excellent electrical properties suggest many potential applications, especially as anodes in lithium batteries and in other conductive textile applications. This work is continuing. We believe that this facile, potentially low-cost method can have much broader applications in other areas as well.

5.2 Future Work

On the basis of work that was conducted in this study, the author would like to propose following future studies:

1. In order to increase the mechanical strength and the electrochemical properities
    - optimize the reaction conditions, such as time, temperature, annealing time, heating rate, and rate of temperature increase
    - optimize the blend ratios of pyrene sulfoinic acid and graphene flakes
    - determine best methods for “soldering” the separated graphene sheets to form a “skin” on the surface to cotton fibers
    - add fillers such as metal and metal oxide particles
    - examine the use of various precursors for carbon fibers such as polyacrylonitrile (PAN), polyvinylchloride (PVC), polyimide (PI), polyamide (PA), pitch, cellulose, and rayon
    - improve the quality of the graphene suspension by examing solvent, surfactant, and preparation method
2. In order to improve the capacitance properties, utilize pore-forming substances (KOH, $ZnCl_2$) to increase the porosity of the graphene-pyrene film.

References

[1] K.S. Novoselov, A.K. Geim, S.V. Morozov, D. Jiang, Y. Zhang, S.V. Dubonos, I.V. Grigorieva, and A.A. Firsov. Science, 2004, 306.

[2] Y. B. Zhang, Y. W. Tan, H. L. Stormer and P. Kim, Nature, 2005, 438, 201.

[3] K. S. Novoselov, Nature, 2005, 438, 197.

[4] Y. Hernandez and V. Nicolosi, Nature Nanotech., 2008, 3, 563.

[5] S.S Li, K.H Tu, C.C. Lin, C.W. Chen and M. Chhowalla. ACS Nano, 2010, 4 , 3169.

[6] H.W. Kim, A.A. Abdala and C. W. Macosko, Macromolecules, 2010, 43, 6515.

[7] J.Q. Liu, L. Tao, W.R. Yang, D. Li, C. Boyer, R. Wuhrer, F. Braet and T. P. Davis, Langmuir, 2010, 26, 10068,

[8] Q. Li, Z.J. Li, M. Chen and Y. Fang, Nano Lett., 2009, 9, 2129,

[9] D.L Son, T. W. Kim, J. H. Shim, J.H. Jung, D.U. Lee, J.M. Lee, W. Park and W. K. Choi Nano. Lett., 2010, 10, 2441,

[10] J. Patil and S. Mann. Adv. Mater, 2009, 21, 2180.

[11] Q.L Bao, H. Zhang, J.X. Yang, S. Wang, D.Y. Tang, R. Jose, S. Ramakrishna, C.T. Lim and K. P. Loh, Adv. Funct. Mater, 2010, 20, 782,

[12] S.M. Paek, E.J. Yoo and I. Honma, Nano Lett., 2009, 9, 72.

[13] E.J. Yoo, J. Kim, E. Hosono, H.S. Zhou, T. Kudo and I. Honma Nano Lett., 2008, 8, 2277.

[14] H.l. Wang, L.F. Cui, Y. Yang, H. S. Casalongue, J.T. Robinson, Y. Liang, Y. Cui, and H.J. Dai. J. Am. Chem. Soc., 2010, 132, 13978.

[15] L. Hu, M. Pasta, F. La Mantia, L.-F. Cui, S. Jeong, H. D. Deshazer, J. W. Choi, S. M. Han, Y. Cui, Nano Lett., 2010, 10, 708.

[16] D. T. Schoen, A. P. Schoen, L. Hu, H.S. Kim, S. C. Heilshorn, Y. Cui, Nano Lett., 2010, 10, 3628.

[17] Q. Su, S.P. Pang, V. Alijani, C. Li, X.L. Feng, K. Mullen, Adv. Mater 2009, 31, 21.

[18] M. Zhang, R. Parajuli, W. Cheung, R. Brukh, H. X. He, Small, 2010, 6, 1100.

[19] M. Yoshio, H.Y. Wang, K. Fukuda, Y. Hara, and Y. Adachic, J. Electrochem. Soc., 2000, 147, 1245.

[20] H.Y. Wang and M. Yoshio, J. Power. Sources., 2001, 93, 123.

[21] E. Peled, C. Menachem, D. Bar-Tow, and A. Melman J. Electro. chem. Soc., 1996, 143, 4.

[22] K. Xu, S.S. Zhang, B. A. Poese, and T. Richard Jow Electrochem. Solid-State Lett., 2002, 5, 259.

[23] D. Bar-Tow,a E. Peled,a and L. Bursteinb, J. Electrochem. Soc., 1999,146,824.

[24] J.C. Yamaki, H. Takatsuji, T. Kawamura and M. Egashira, Solid State Ionics, 2002, 148, 241.

[25] J. R. Dahn, T. Zheng, Y. H. Liu and J. S. Xue, Science, 1995, 270, 590.

[26] K. Sato, M. Noguchi, A. Demachi, N. Oki and M. Endo, Science, 1994, 264, 556.

[27] B. Scrosati, Electrochimica Acta, 2000, 45, 2461.

[28] W. V. Schalkwijk and B. Scrosati, Chemistry and Materials Science, 2002, 1-5.

[29] M. S. Whittingham, Chem. Rev. 2004, 104, 4271.

[30] S. Megahed and W. Ebner, Journal of Power Sources, 1995, 54, 155.

[31] J. Chen, J. Z. Wang, A. I. Minett, Y. Liu, C. Lynam, H. K. Liu and G. G. Wallace, Energy Environ. Sci., 2009, 2, 393.

[32] Electronics lab, advertisement http://www.electronicslab.com/articles/Li_Ion_reconstruct/, 2011

[33] G. Jeong, Y. U. Kim, H. Kim, Y. J. Kim and H. J. Sohn, Energy Environ. Sci., 2011, 4, 1986.

[34] S. Iijima, Nature, 1991, 354, 56.

[35] G. Maurin, C. Bousquet, F. Henn, P. Bernier, R. Almairac and B. Simon, Chem. Phys. Lett., 1999, 312, 14.

[36] B. Gao, A. Kleinhammes, X. P. Tang, C. Bower, L. Fleming, Y. Wu and O. Zhou, Chem. Phys. Lett., 1999, 307, 153.

[37] V. A. Nalimova, D. E. Sklovsky, G. N. Bondarenko, H. AlvergnatGaucher, S. Bonnamy and F. Beguin, Synth. Met., 1997, 88, 89.

[38] Rhône-Alpes competence center in nanoscience <http://www.cnano-rhone-alpes.org>

[39] B. Gao, C. Bower, J. D. Lorentzen, L. Fleming, A. Kleinhammes, X. P. Tang, L. E. McNeil, Y. Wu and O. Zhou, Chem. Phys. Lett., 2000, 327, 69.

[40] J. Y. Eom, H. S. Kwon, J. Liu and O. Zhou, Carbon, 2004, 42, 2589.

[41] X. X. Wang, J. N. Wang, H. Chang and Y. F. Zhang, Adv. Funct. Mater., 2007, 17, 3613.

[42] C. H. Mi, G. S. Cao and X. B. Zhao, J. Electroanal. Chem., 2004, 562, 217.

[43] C. C. Li, X. M. Yin, L. B. Chen, Q. H. Li and T. H. Wang, J. Phys. Chem. C, 2009, 113, 13438.

[44] L. W. Ji and X. Zhang, Nanotechnology, 2009, 20, 155705.

[45] V. Subramanian, H. W. Zhu and B. Q. Wei, J. Phys. Chem. B, 2006, 110, 7178.

[46] http://en.wikipedia.org/wiki/Graphene

[47] M. J. Allen, V. C. Tung and R. B. Kaner, Chem. Rev., 2010, 110, 132.

[48] Y. Shao, J. Wang, H Wu, J. Liu, I. A. Aksay, Y. Lin, Electroanalysis, 2010, 22, 1027.

[49] J. T. Robinson, S. M. Tabakman, Y Liang, H Wang, H. S. Casalongue, D. Vinh, and H. Dai J. Am. Chem. Soc., 2011, 133, 6825.

[50] X.M Sun, Z. Liu, K. Welsher, J.T. Robinson, A. Goodwin, S. Zaric, and H.J. Dai, Nano Res, 2008, 1, 212.

[51] L.Z. Feng and Z. Liu, Nanomedicine , 2011, 6, 317.

[52] F. Ji, Y. L. Li, J. M. Feng, D. Su, Y. Y. Wen, Y. Feng and F. Hou, J. Mater. Chem., 2009, 19, 75.

[53] M. H. Liang and L. J. Zhi, J. Mater. Chem., 2009, 19, 5871.

[54] D. Chen, L. H. Tang and J. H. Li, Chem. Soc. Rev., 2010, 39, 3157.

[55] A. V. Murugan, T. Muraliganth and A. Manthiram, J. Phys. Chem. C, 2008, 112, 14665.

[56] E. Yoo, J. Kim, E. Hosono, H. Zhou, T. Kudo and I. Honma, Nano Lett., 2008, 8, 2277.

[57] M. Yoo, C. W. Frank, S. Mori and S. Yamaguchi, Chem. Mater., 2004, 16, 1945.

[58] S. W. Woo, K. Dokko, H. Nakano and K. Kanamura, Electrochemistry, 2007, 75, 635.

[59] Y. S. Hu, P. Adelhelm, B. M. Smarsly, S. Hore, M. Antonietti and J. Maier, Adv. Funct. Mater., 2007, 17, 1873.

[60] G. K. Dimitrakakis, E. Tylianakisa and G. E. Froudakis, Nano. Lett., 2008, 8, 3166.

[61] C. J. Meyers, S. D. Shah, S. C. Patel, R. M. Sneeringer, C. A. Bessel, N. R. Dollahon, R. A. Leising and E. S. Takeuchi, J. Phys. Chem. B, 2001, 105, 2143.

[62] T. Wang, X. Y. Liu, D. Y. Zhao and Z. Y. Jiang, Chem. Phys. Lett., 2004, 389, 327.

[63] H. S. Zhou, S. M. Zhu, M. Hibino, I. Honma and M. Ichihara, Adv. Mater., 2003, 15, 2107.

[64] F. B. Su, X. S. Zhao, Y. Wang, J. H. Zeng, Z. C. Zhou and J. Y. Lee, J. Phys. Chem. B, 2005, 109, 20200.

[65] K. T. Lee, J. C. Lytle, N. S. Ergang, S. M. Oh and A. Stein, Adv. Funct. Mater., 2005, 15, 547.

[66] H.Y. Lee and S.M. Lee, Electrochemistry Communications., 2004, 6, 465.

[67] M. Yoshio, H.Y. Wang, K. Fukuda, T. Umeno, N. Dimov, and Z. Ogumib J. Electrochem. Soc., 2002, 149, 1598.

[68] Z.S. Wena, J. Yang, B.F. Wanga, K. Wanga and Y. Liua, Electrochemistry Communications,2003, 5, 165.

[69] B. Veeraraghavan, A. Durairajan, B. Haran, B. Popov, and R. Guidotti, J. Electrochem. Soc., 2002, 149, 675.

[70] G.X. Wang, J. Yao, J.H. Ahn, H.K. Liu and S.X. Dou, Journal of Applied Electrochemistry ,2004, 34, 187.

[71] Z.S. Wu, W.C. Ren, L. Wen, L.B. Gao, J.P. Zhao, Z.P. Chen, G.M. Zhou, F. Li and H.M. Cheng, ACS Nano, 2010, 4 , 3187.

[72] D.H. Wang, D. Choi, J. Li, Z.G. Yang, Z.M. Nie, R. Kou, D.H. Hu, C.M. Wang, L. V. Saraf, J.G. Zhang, I. A. Aksay and J. Liu, ACS Nano, 2009, 3 , 907.

[73] G.M. Zhou, D.W. Wang, F. Li, L.L. Zhang, N. Li, Z.S. Wu, L. Wen, G. Q. Lu, and H.M. Cheng, Chem. Mater., 2010, 22, 5306.

[74] P. Lian, X.F. Zhu, H.F. Xiang, Z. Li, W.S. Yang and H.H. Wang, Electrochimica Acta, 2010, 56, 834.

[75] C.J. Kim, M. Noh, M. Choi, J. Cho, and B. Park, Chem. Mater., 2005, 17 , 3297.

[76] J. Yao, X.P. Shen, B. Wang, H.K. Liu and G.X. Wang, Electrochemistry Communications , 2009, 11, 1849-1852

[77]S. M. Paek, E. Yoo and I. Honma, Nano Lett., 2009, 9, 72.

[78] D. A. Dikin, S. Stankovich, E. J. Zimney, R. D. Piner, G. H. B. Dommett, G. Evmenenko, S. T. Nguyen and R. S. Ruoff, Nature 448, 457.

[79] C. Virojanadara, M. Syväjarvi, R. Yakimova, and L. I. Johansson, Phys. Rev. B, 2008, 78, 245.

[80] S. Stankovich, D. A. Dikin, R. D. Piner, K. A. Kohlhaas, A. Kleinhammesc, Y.Y. Jia, Y. Wu, S. T. Nguyen, and R. S. Ruoff, Carbon, 2007, 45, 1558.

[81] V.R. Silvia, J. I. Paredes, M.A. Amelia and J. M. D. Tascón , J. Mater. Chem., 2009, 19, 3591.

[82] W.X. Zhang, J.C. Cui, C.A. Tao, Y.G. Wu, Z.P. Li, L. Ma, Y.Q. Wen, G.T. Li,Angewandte Chemie, 2009, 121, 5978.

[83] Z.T. Luo, Y. Lu, L. A. Somers and A. T. Charlie Johnson, J. Am. Chem. Soc., 2009, 131, 898.

[84] D. Graf, F. Molitor, K. Ensslin, C. Stampfer, A. Jungen, C. Hierold, and L. Wirtz, Nano Lett., 2007, 7 , 238.

[85] A. V. Murugan, T. Muraliganth and A. Manthiram, J. Phys. Chem. C, 2008, 112, 14665.

[86] D. Chen, L. H. Tang and J. H. Li, Chem. Soc. Rev., 2010, 39, 3157.

[87] M. Yoo, C. W. Frank, S. Mori and S. Yamaguchi, Chem. Mater., 2004, 16, 1945.

[88] F. Ji, Y. L. Li, J. M. Feng, D. Su, Y. Y. Wen, Y. Feng and F. Hou, J. Mater. Chem., 2009, 19, 9063.

[89] M. H. Liang and L. J. Zhi, J. Mater. Chem., 2009, 19, 5871.

[90] http://en.wikipedia.org/

[91] "Study Sizes up Nanomaterial Toxicity". Chemical & Engineering News 86 (35). 1 Sep 2008.

[92] M. Endo, K. Takeuchi, S. Igarashi, K. Kobori, M. Shiraishi and H. W. Kroto, Journal of Physics and Chemistry of Solids,1993, 54, 1841

[93] F. G. Gonon, C. M. Fombarlet, M. J. Buda, J. F. Pujol Anal. Chem., 1981, 53, 1386.

[94] F. G. Gonon, C. M. Fombarlet, M. J. Buda and J. F. Pujol Anal, Chem., 1981, 53, 1386.

[95]M. Endo, K. Takeuchi, K. Kobori, K. Takahashi, H. W. Kroto and A. Sarkar, Carbon, 1995, 33, 873.

[96] D. Stephen, Beckenbaugh, D. Robert, Redondo, Jacqueline, Popich, S. Laura , Klawitter, J. Linscheid, L. Ronald, The Journal of Bone and Joint Surgery , 1999, 81, 635.

[97]Y. S. Han, and J. Y. Lee, Electrochimica Acta, 2003, 48, 1073.

[98] H. L. Zhanga, S. H. Liua, F. Lia, S. Baia, C. Liua, J. Tana and H. M. Cheng, Carbon, 2006, 44, 2212.

[99] Y.F. Zhoua, b, S. Xiea and C.H. Chen, Electrochimica Acta, 2005, 50, 4728,

[100] J. F. Evans, and T. K. Anal, Chem., 1977, 49, 1632.

[101] Y. S. Han, J. H. Jung, and J. Y. Leec J., Electrochem.,Soc., 2004, 151, A291,

[102] L.W. Ji and X.W Zhang, Energy Environ. Sci., 2010, 3, 124.

[103] Y. Xu, H. Bai, G. Lu, G. Q. Shi, J. Am. Chem. Soc. 2008, 130, 5856.

[104] C. Ehli, G. M. A. Rahman, N. Jux, D. Balbinot, D. M. Guldi, F. Paolucci, M. Marcaccio, D. Paolucci, M. Melle-Franco, F. Zerbetto, S. Campidelli, M. Prato, J. Am. Chem. Soc. 2006, 128, 11222.

[105] K. M. Borysenko, J. T. Mullen, X. Li,1 Y. G. Semenov,1 J. M. Zavada,1 M. Buongiorno Nardelli and K. W. Kim, Phys. Rev. B, 2011, 83, 161402.

[106] C.Y Wang, D. Li, C.O. Too and G.G. Wallace. Chem. Mater., 2009, 21, 2604.